Catalysis Today 150 (2010) 55–60

Contents lists available at ScienceDirect

Catalysis Today

journal homepage: www.elsevier.com/locate/cattod

Long carbon nanotubes intercrossed Cu/Zn/Al/Zr catalyst for CO/CO_2 hydrogenation to methanol/dimethyl ether

Qiang Zhang, Yi-Zan Zuo, Ming-Han Han, Jin-Fu Wang, Yong Jin, Fei Wei *

Beijing Key Laboratory of Green Chemical Reaction Engineering and Technology, Department of Chemical Engineering, Tsinghua University, Beijing 100084, China

ARTICLE INFO

Article history:
Available online 23 June 2009

Keywords:
Carbon nanotube
Cu/Zn/Al/Zr catalyst
CO/CO_2 hydrogenation
Methanol synthesis
Dimethyl ether synthesis
Stability

ABSTRACT

Vertically aligned carbon nanotube (CNT) arrays were dispersed in Na_2CO_3 solution and co-precipitated with metal nitrite to form long CNTs (over 500 μm) intercrossed Cu/Zn/Al/Zr catalyst (CD703). The catalyst was used for methanol synthesis from CO/CO_2 hydrogenation. The space time yield (STY) of methanol on CD703 increased to 0.94 and 0.28 g/(gcat h), with an increment of 7% and 8% compared with that on the Cu/Zn/Al/Zr catalyst without CNTs for CO and CO_2 hydrogenation, respectively. Furthermore, when combined with γ-Al_2O_3 catalyst and HZSM-5, dimethyl ether (DME) was obtained with a STY of 0.90 and 0.077 g/(gcat h) at 270 °C from one step CO and CO_2 hydrogenation, respectively. Due to the phase separation, ion doping and valence compensation, hydrogen reversibly adsorption and storage on CNTs promoting hydrogen spillover, CD703 catalyst show good activity for methanol synthesis. Owing to the high thermal conductivity of CNTs, the stability of CD703 was improved. This indicated that long CNTs were a good promoter on the Cu/Zn/Al/Zr catalyst for methanol/DME production from CO/CO_2 hydrogenation.

1. Introduction

It is a long history for methanol production from CO hydrogenation in industry on Cu/Zn/Al catalyst [1–4]. To promote the methanol synthesis process, CO_2 was always added into the reactant for methanol synthesis [5–7]. Recently, the greenhouse effect is a threat to the living environment of mankind. The transformation of CO_2 into useful chemicals, e.g. methanol, dimethyl ether (DME), is an attractive way to protect global environment. However, the conventional Cu/Zn/Al catalyst is a porous solid catalyst with low thermal conductivity. The reaction heat is difficult to be transferred and the diameter of single tube of the reactor has to be limited to several centimeters in order to control the temperature of the hot spots in the fixed bed. Meanwhile, the Cu/Zn/Al catalyst is not as active for methanol synthesis from a H_2/CO_2 mixture at temperatures below 250 °C [2,4], even though it is now accepted that methanol synthesis from syngas actually proceeds through CO_2 hydrogenation. A highly active and stable catalyst is needed.

The Cu/Zn/Al catalysts for methanol synthesis are agglomerated nanoparticles [8–10]. The good Cu/Zn dispersion is believed to be a key factor for a high-performance methanol synthesis catalyst [2,4,11,12]. Most researches are concerned on modifications of conventional Cu/Zn/Al methanol synthesis catalysts. Some works sought to improve the dispersion of the conventional Cu/Zn/Al catalyst by using complicated preparation procedures. Other works sought to improve the catalyst by adding additives other than Al to Cu/Zn crystallites or Cu/Zn/Al composites, e.g., Melian-Cabrera reported the use of Cr, Zr, V, Ce, Ti, Ga, and Pd to modify Cu/ZnO-based catalysts [13–16]. Some additives, such as Ce, Ga, Pd, were quite expensive. Recently, we found that the catalyst performance can be enhanced by the catalyst structure modulation with doping Zr [17]. By using a well controlled co-precipitation procedure, Cu/Zn/Al/Zr catalyst with high activity for both CO and CO_2 hydrogenation was developed. Furthermore, the object to obtain a catalyst with high activity and stability is still a goal. The viewpoint of enhancing heat transfer on Cu/Zn-based catalyst to promote methanol synthesis is still less mentioned.

Carbon nanotubes (CNTs) were found to possess excellent thermal conduction property. For example, the axial thermal conductivity of CNTs was found to be extremely high, about 2000 W/m K or more than 3000 W/m K for multi-walled CNTs and even higher for single-walled CNTs [18,19], and the thermal conductivities of CNT-in-oil suspensions and CNT-in-polymer composites were observed to be significantly improved. For example, a 150% increase at 1% volume fraction of CNTs [20,21]. Some trials have been done on CNTs-Cu/Zn/Al catalyst [12,22]. Although short agglomerated CNTs wherein the nanotubes are randomly entangled with each other were used in previous research, the CNT promotion effect was remarkable on Cu/Zn/Al

* Corresponding author. Tel.: +86 10 62784654; fax: +86 10 62772051.
E-mail address: weifei@flotu.org (F. Wei).

0920-5861/$ – see front matter © 2009 Elsevier B.V. All rights reserved.
doi:10.1016/j.cattod.2009.05.018

catalyst for methanol synthesis [12]. Now, millimeter vertically aligned CNT arrays were large-scaled produced on ceramic spheres [23–25]. They are easily to be dispersed into fluffy CNTs by high speed shearing [26]. CNTs also showed amazing applications in catalysis [27–29]. With larger aspect ratio, the CNTs showed better performance in heat transfer. Till now, the performance of long CNTs intercrossed Cu/Zn/Al/Zr catalyst for CO/CO_2 hydrogenation is still an open question.

Herein, super long CNTs were dispersed into Cu/Zn/Al/Zr catalyst. The improved catalyst was used for direct CO/CO_2 hydrogenate into methanol. It was combined with γ-Al_2O_3 or HZSM-5 for DME production from CO/CO_2 hydrogenation.

2. Experimental

The vertically aligned CNT arrays with a length of 5.0 mm were obtained through a floating catalyst process (Fig. 1a) [30]. They are with good alignment as shown in Fig. 1b. It was dispersed by high speed shearing [26] and then mild acid treatment. The length of the as-treated CNTs was over 500 μm, which can be dispersed easily into the Na_2CO_3 solution by high speed shearing in liquid phase. Furthermore, the solution of $Cu(NO_3)_2{\cdot}6H_2O$, $Zn(NO_3)_2{\cdot}6H_2O$, $Al(NO_3)_3{\cdot}6H_2O$ and $ZrOCl_2$ with a concentration of 0.6 mol/L were mixed with a ratio of 6:3:0.5:0.5, then the mixture was precipitated with the $CNTs/Na_2CO_3$ solution at 80 °C with strong stirring for 1.0 h. After filtration and washing, the catalyst was dried at 120 °C for 12.0 h and calcined at 300 °C for 4.0 h to get the long CNTs intercrossed Cu/Zn/Al/Zr catalyst (CD703).

As a reference catalyst, the Cu/Zn/Al/Zr catalyst (CD503) with a ratio Cu:Zn:Al:Zr of 6:3:0.5:0.5 was synthesized by co-precipitation methods [17]. Also a commercial catalyst code named COM that had been successfully used in many plants in China for producing methanol from syngas was used. There have been many generations of commercial catalysts for methanol synthesis, and this is perhaps the most commonly used industrial catalyst in China at present [17,31].

For DME synthesis from CO, γ-Al_2O_3 was used as the methanol dehydrated catalyst. While for DME synthesis from CO_2, HZSM-5

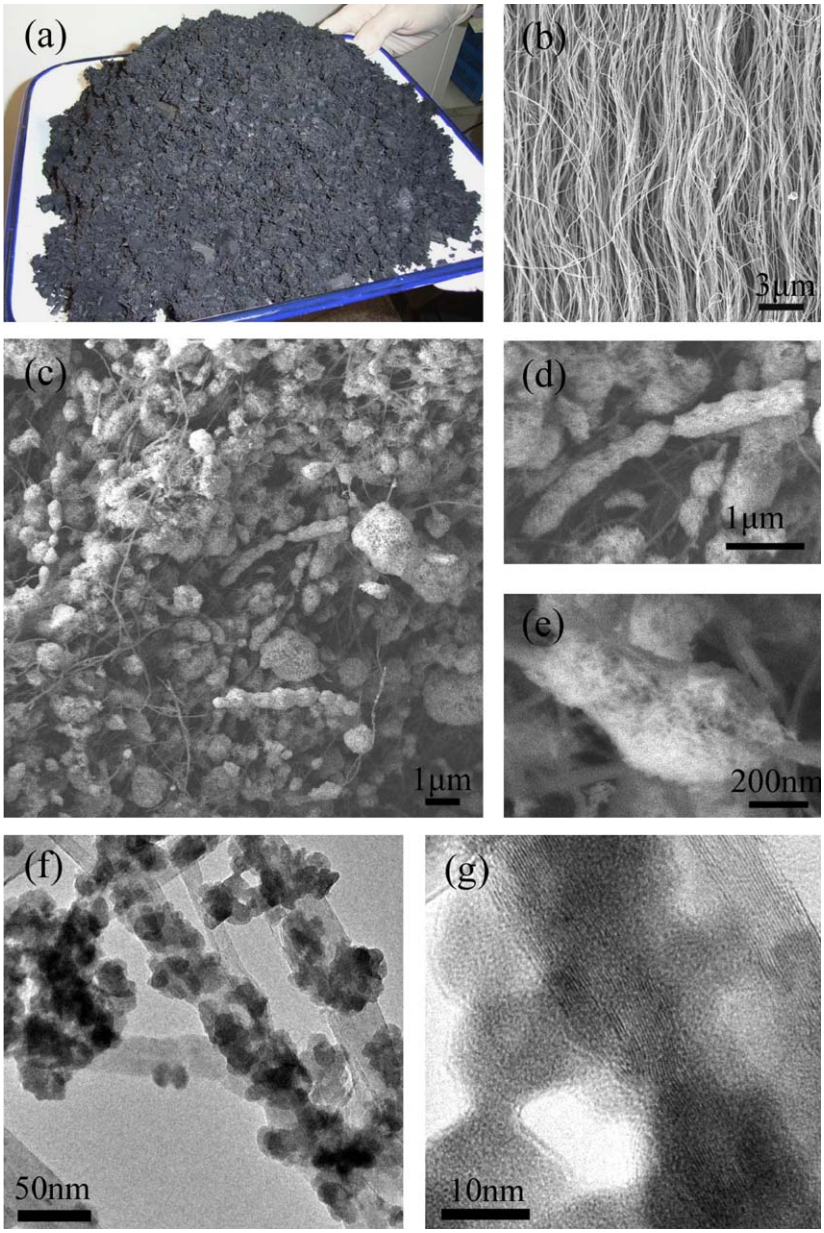

Fig. 1. (a) Large amount of vertically aligned CNT arrays. (b) SEM images of CNTs in the array with good alignment. (c)–(e) SEM images, (f) TEM image and (g) high-resolution TEM images of long CNT intercrossed Cu/Zn/Al/Zr catalyst (CD703).

with a Si/Al ratio of 39 was used for methanol dehydration. The bifunctional DME synthesis catalysts were physical mixtures of methanol synthesis catalyst and dehydrated catalyst with the ratio of 2.0.

The catalytic reaction on the COM/CD503/CD703 catalyst was carried out in a fixed bed reactor. The reactor is with a diameter of 12.0 mm and a length of 500 mm. Before the reaction started, the catalyst was reduced with a 5% H_2/95% N_2 mixture at atmospheric pressure by raising the temperature slowly to the reaction temperature over 10.0 h. Then the reduction gas was switched to the reaction gas and the pressure was raised to the reaction pressure 4.0 MPa to start the reaction. The space velocity was 6000 mL/(gcat h). The first sample of the effluent was taken 2.0 h after steady reaction conditions were established, and then samples were taken every 30 min for online analysis of the effluent composition. The reaction temperature was controlled by furnace heating device and the pressure was controlled by the feeding rate. For CO hydrogenation into methanol, the ratio of H_2 to CO (5% CO_2 was included) was 2.0, the temperature was 230 °C. For CO_2 hydrogenation into methanol, the ratio of H_2 to CO_2 was 3.0, the temperature was 240 °C. DME can be obtained from CO hydrogenation using CD703 combined with γ-Al_2O_3 catalyst, the ratio of H_2 to CO was 2.0. DME synthesis can also be synthesized from CO_2 hydrogenation using CD703 combined with HZSM-5 catalyst. The ratio of H_2 to CO_2 was 3.0, the pressure was 5.0 MPa.

The morphology of the catalyst was characterized by a JSM 7401F scanning electron microscope (SEM) operated at 5.0 kV and a JEM 2010 high-resolution transmission electron microscope (TEM) operated at 120.0 kV. The sample for the TEM observation was prepared using a common sonication method. The structure of the catalyst was identified by the X-ray powder diffractometer (XRD, D8-Advance, Bruker, Germany) using Cu K_α radiation, a fixed power source (40.0 kV, 40.0 mA), and an aligned silicon detector.

The reactor was connected to an online GC 7890II gas chromatograph with a thermal conductivity detector, and a Porapak T (5.0 m) column connected in parallel with a TDX-01 (3.0 m) column. CO, CO_2 conversion, the space time yields (STYs) of DME and MeOH, which gave the amounts of DME and MeOH produced per gram catalyst per second, were defined as follows:

$$X_{CO} = \frac{n_{CO,in} - n_{CO,out}}{n_{CO,in}} \quad (1)$$

$$X_{CO_2} = \frac{n_{CO_2,in} - n_{CO_2,out}}{n_{CO_2,in}} \quad (2)$$

$$STY_{DME} = \frac{n_{DME,out}}{n_{CO/CO_2,in}} \times SV_{CO/CO_2} \times M_{DME} \times 0.001\ (kg/g)/22.4\ (L/mol)/2 \quad (3)$$

$$STY_{MeOH} = \frac{n_{CH_3OH,out}}{n_{CO/CO_2,in}} \times SV_{CO/CO_2} \times M_{MeOH} \times 0.001\ (kg/g)/22.4\ (L/mol) \quad (4)$$

where n_{DME}, n_{CO} and n_{CO_2} were the molar flow rates of DME, CO, and CO_2, respectively; SV_{CO/CO_2} was the space velocity of CO or CO_2; and M_{DME} and M_{MeOH} were the molar mass of DME and MeOH, respectively.

3. Results and discussion

3.1. The morphology of CNTs intercrossed Cu/Zn/Al/Zr catalyst

After co-precipitation process, a CNT (15 wt%) intercrossed Cu/Zn/Al/Zr catalyst (CD703) was obtained. As shown in Fig. 1c, the long CNTs were interwoven into a 3D network in the catalyst agglomerates. The long CNTs were coated by the Cu/Zn/Al/Zr catalyst, and a necklace-like hybrid structure was shown in Fig. 1c. The size of Cu/Zn/Al/Zr agglomerates was just 300–600 nm in diameter. As shown in Fig. 1d and e, the Cu/Zn/Al/Zr nanoparticles were dispersed among CNTs networks. As can been seen in TEM images of CD703 catalyst (Fig. 1f and g), although some large Cu/Zn/Al/Zr agglomerates are formed on the CNT network during sonication process, a majority of catalyst particles distributed along CNTs possessed a size of 12–16 nm. The reference catalysts are nanoparticle agglomerates, the morphology of which can be found in Supplementary material. The XRD patterns of COM, CD503, CD703 catalysts were shown in Fig. 2. The CD703 pattern showed low signal–noise ratio and weak peak intensity. CuO peak and MWCNT peak can be detected. The weak peaks in CD503 XRD pattern are assigned to CuO. For COM catalyst, the peak patterns were assigned to CuO and ZnO with good crystalline. The high peak intensity of COM catalyst was high and small half-peak width indicated the relatively large crystalline size of CuO and ZnO. Compared with COM catalyst, the CuZn dispersion in CD703 is much better [32].

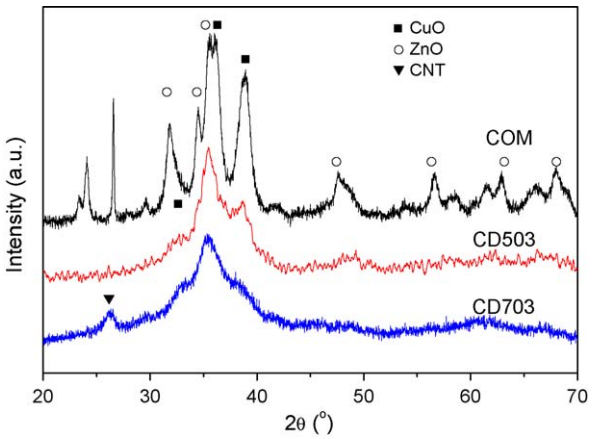

Fig. 2. XRD patterns of COM, CD503 and CD703 catalyst.

3.2. The activity of methanol synthesis from CO/CO_2 hydrogenation

Methanol synthesis was tested from CO or CO_2 hydrogenation and the typical results were shown in Table 1. On CD503 catalyst, the CO conversion was 0.509, and the STY of methanol was about 0.877 g/(gcat h). When long CNTs were added, the CO conversion and STY of methanol increased to 0.545 and 0.939, respectively. Compared with CO conversion on CD503 catalyst and COM catalyst, there was a 7% and 33.5% increment. For CO_2 hydrogenation, the CO_2 conversion was just 0.215 when CD703 catalyst served as catalyst for methanol synthesis. Compared with CO_2 hydrogenation on CD503 and COM catalyst, CO_2 conversion was increased by a 4.8% and 31.2%, respectively.

Table 1
Methanol synthesis from CO or CO_2 hydrogenation on various catalysts.

Catalyst	CO hydrogenation		CO_2 hydrogenation	
	CO conversion	STY g/(gcat h)	CO_2 conversion	STY g/(gcat h)
COM	0.408	0.707	0.163	0.151
CD503	0.509	0.877	0.205	0.261
CD703	0.545	0.939	0.215	0.282

3.3. The activity of DME synthesis from CO/CO_2 hydrogenation

For DME one-step synthesis from CO/CO_2 and H_2, there are four independent stoichiometric reactions, namely,

- Methanol synthesis from CO hydrogenation:

$$CO + 2H_2 = CH_3OH \quad -90.4\,kJ\,mol^{-1} \tag{5}$$

- Methanol synthesis from CO_2 hydrogenation:

$$CO_2 + 3H_2 = CH_3OH + H_2O \quad -49.3\,kJ\,mol^{-1} \tag{6}$$

- Water gas shift reaction:

$$CO + H_2O = CO_2 + H_2 \quad -41.0\,kJ\,mol^{-1} \tag{7}$$

- DME synthesis from methanol dehydration:

$$2CH_3OH = CH_3OCH_3 + H_2O \quad -23.4\,kJ\,mol^{-1} \tag{8}$$

Cu/Zn-based catalyst served as catalyst in methanol synthesis process as shown in (5) and (6). DME can be easily obtained by methanol dehydration with γ-Al_2O_3 or HZSM-5 as catalyst [33]. Here, we mixed γ-Al_2O_3 and CD703 catalyst, and tested DME synthesis from CO hydrogenation. To show the effect of the addition of CNTs, a CD503 catalyst combined with γ-Al_2O_3 catalyst was also tested. Fig. 3 shows curve of the CO conversion, STY of methanol, and DME vs reaction temperature from CO hydrogenation. The CO conversion and STY of DME increased with higher temperature. The methanol produced on CD703 exhibited the highest yield at a temperature of 230 °C. The CO conversion, STY of methanol and DME all increased when 15 wt% CNTs were added into the Cu/Zr/Al/Zr catalyst. At low temperature, there were increases of CO conversion and STY of methanol. When the reaction temperature became higher, the increment of CO conversion and methanol STY became smaller.

Using CD703 + HZSM-5 catalyst, DME can be obtained from CO_2 hydrogenation. As shown in Fig. 4, with higher reaction temperature, the conversion of CO_2 and STY of DME and methanol simultaneously increased. There was about 1% increment for the CO_2 conversion during all the temperature range.

3.4. The stability of DME synthesis from CO hydrogenation

The stability is a key issue for one step DME synthesis from syngas. Usually, the sintering was a main factor for the deactivation of CuZn-based catalyst. Cu/Zn particles will cluster into large particles through Ostwald ripening or migration, and the activity for methanol synthesis decreases gradually [2,4,7,34,35]. To show the stability of the CNTs intercrossed catalyst, a 160-h test for CO hydrogenation on CD703 + γ-Al_2O_3 catalyst with a reaction pressure of 5.0 MPa was carried out. As comparison, CD503 with no CNTs was taken as reference. As shown in Fig. 5, during the initial 8.0 h, the CO conversion and DME STY were higher on the CD503 catalyst than those on CD703 catalyst. However, the deactivated rate on the CD503 was fast. Then, CO conversion and STY of DME turn opposite position after 8.0-h reaction. CO conversion decreased by 5% and 2%; STY of DME decreased by 13% and 2% on CD503 and CD703 catalyst, respectively. The stability of DME synthesis on the CD703 catalyst was improved when long CNTs were added.

3.5. The promotion of long CNTs on CO/CO_2 hydrogenation

Long CNTs were added into the Cu/Zn/Al/Zr catalyst for methanol synthesis. In CD703, with the addition of long CNTs, as indicated by the XRD pattern as shown in Figs. 1 and 2, a Cu/Zn/Al/Zr catalyst with high Cu/Zn dispersion was formed with the contribution of heterogeneous nucleation. Liu et al. reported that the Zr^{4+} dissolved in ZnO crystal caused the formation of positive ion defects on the surface of Cu–ZnO. These defects can form and stabilize more active sites, Cu^0–Cu^+–O–Zn^{2+}, on the catalyst surface by adsorbing Cu^+ [36] and the Cu/Zn dispersion was thereby improved by Zr doping. Furthermore, there were phase separation effect originated from the CNT intercrossed Cu/Zn/Al/Zr particles. As reported by Dong et al., the addition of CNTs can increase specific surface area, especially Cu surface area of the catalyst, and CNTs can reversibly adsorb and store a considerably greater amount of hydrogen [12]. The above mentioned feature was beneficial for generating microenvironments with high stationary-state concentration of active hydrogen adspecies on the surface of the CNT promoted Cu/Zn/Al/Zr catalyst [12]. Here, the CNTs from arrays with large aspect ratio and good dispersion were intercrossed among the methanol synthesis catalysts, and the highly conductive CNTs might promote hydrogen spillover from the Cu sites to the Cu/Zn interfacial active sites [12]. These characteristics were favorable for increasing the rate of the CO/CO_2 hydrogenation into methanol (Table 1). With faster rate of methanol production on CD703, DME was also available with high STY (Figs. 3 and 4).

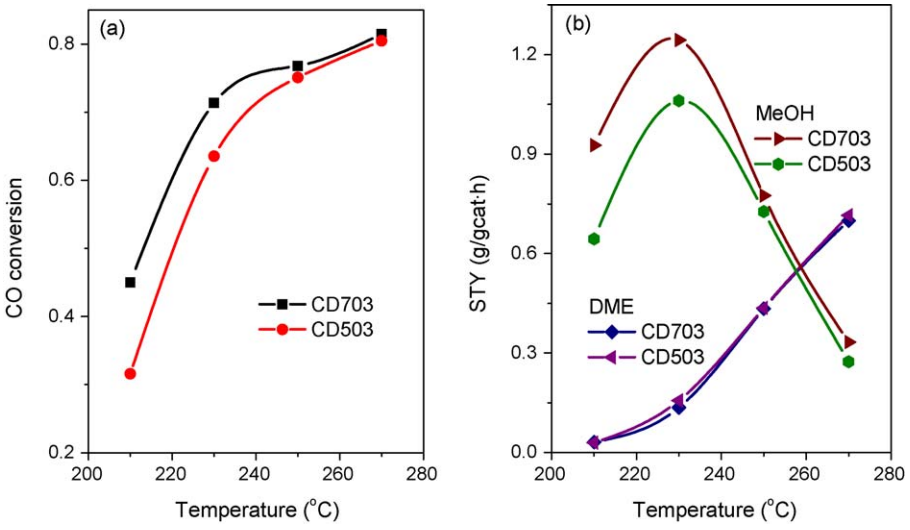

Fig. 3. (a) CO conversion and (b) STY yield of methanol and DME on CD503/CD703 + γ-Al_2O_3 catalyst.

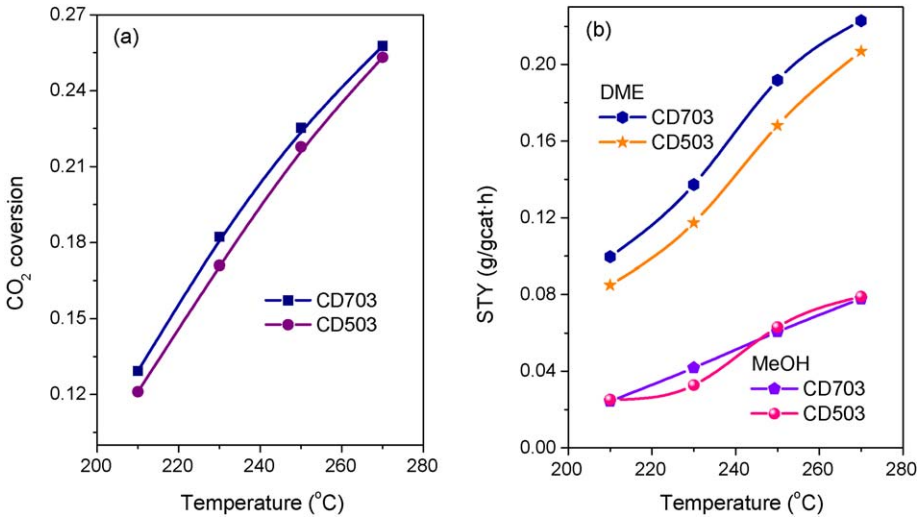

Fig. 4. (a) CO_2 conversion and (b) STY yield of methanol and DME on CD503/CD703 + HZSM-5 catalyst.

The stability of the CD703 is another key issue, especially for DME production. It is an important issue for industrial applications. When CD703 catalyst used in the fixed bed, it should be granulated into cylindrical, trefoil or spherical particles. If the temperature was higher than 400 °C, the Cu/Zn would sinter into large catalyst particles and the deactivation is irreversible. To estimate the heat transfer phenomena in a single particle, the heat transfer in a control volume of the present catalyst can be described by:

$$4\pi(r+dr)^2\lambda_P\frac{d}{dr}\left(T+\frac{dT}{dr}dr\right)-4\pi r^2\lambda_P\frac{dT}{dr}=4\pi r^2 dr k_v C\Delta H \quad (9)$$

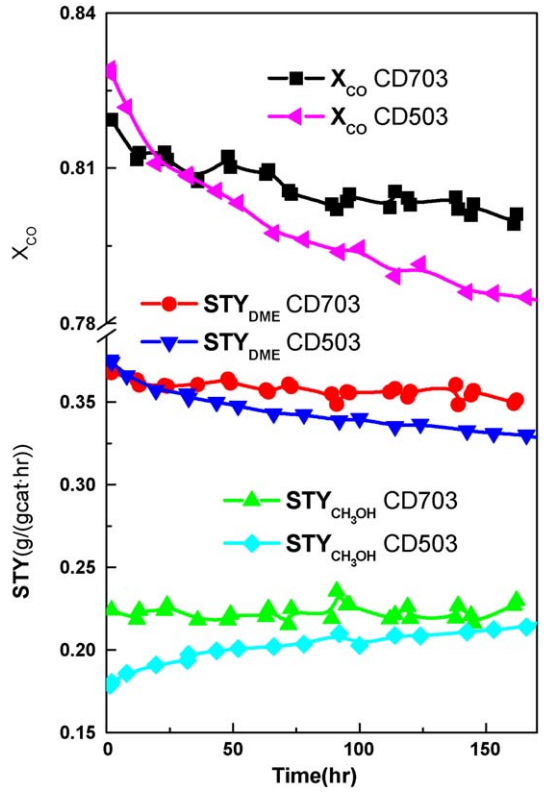

Fig. 5. Comparison of CD503/CD703 + γ-Al_2O_3 catalyst for CO hydrogenation into DME.

where λ_P is thermal conductivity of the catalyst, ΔH is the enthalpy of methanol synthesis. After deduction on the homogeneous spherical catalyst particles, Eq. (9) can be transformed into:

$$\frac{d^2T}{dr^2}+\frac{2}{r}\frac{dT}{dr}=C^m\frac{\Delta H}{\lambda_P} \quad (10)$$

The boundary condition can be further described by:

$$r=0,\quad \frac{dT}{dr}=0 \quad (11)$$

$$r=R,\quad T=T_s \quad (12)$$

Thus, the highest temperature difference in a single particle can be expressed by:

$$T-T_s=\frac{\Delta H\cdot D_e}{\lambda}(C_A-C_{As}) \quad (13)$$

The highest temperature difference is obtained by the assumption that the concentration was zero in the particles. From Eq. (13), it is indicated that the temperature rise in the single particle is inversely proportion to the conductivity of the catalyst. For CD503, the porous catalyst similar to traditional Cu/Zn/Al catalyst, the thermal conductivity was about 0.4 W/m K [37]. In CD703, CNTs were long and woven into a continuous phase. With previous model by Nan et al. [38,39], the thermal conductivity was estimated to be 20 W/m K. This was similar to the results obtained in CNTs/ceramic or CNTs polymer system in the literature [40–42]. With a high thermal conductive supports, the heat produced by the reaction can be removed quickly and the maximum temperature rise decreased from 50 to 1 °C (in CO hydrogenation with D_e of 6.2×10^{-6} m^2/s [37]) in CD703. Furthermore, the catalyst nanoparticles in CD703 are distributed among CNT network (Fig. 1) and the sinter of Cu/Zn particles on CD703 was thereby suppressed compared with COM or CD503 catalyst (Fig. 5). By the design of hierarchical structure of the catalyst, a high thermal conductive catalyst with high Cu/Zn dispersion was obtained (Fig. 5), leading to the relatively high activity and stability in the reaction.

4. Conclusions

By co-precipitation methods, long CNTs from vertically aligned CNT arrays were dispersed and intercrossed into Cu/Zn/Al/Zr catalyst (CD703) for methanol/DME production through CO/CO_2 hydrogenation. The CNTs were coated by Cu/Zn/Al/Zr catalyst

particles. With the effect of phase separation, ion doping and valence compensation, hydrogen reversibly adsorption and storage on CNTs promoting hydrogen spillover, the CNT promoted catalyst showed high performance for methanol synthesis. For CO/CO_2 hydrogenation, the STY of methanol on CD703 increased to 0.94 and 0.28 g/(gcat h), with an increment of 7% and 8% compared to Cu/Zn/Al/Zr catalyst without CNTs (CD503). When CD 703 was combined with γ-Al_2O_3 catalyst and HZSM-5, DME was obtained with a STY of 0.90 and 0.077 g/(gcat h) at 270 °C from one step CO hydrogenation and CO_2 hydrogenation. Meanwhile, the thermal conductivity increased from 0.4 to 20 W/m K, and thus the hot spot in the catalyst was eliminated, preventing the catalyst from deactivation. The long CNT was an extraordinary promoter when it was intercrossed into Cu/Zn/Al/Zr catalyst for methanol synthesis.

Acknowledgements

The work was supported by the Foundation for Natural Scientific Foundation of China (Nos. 20736004 and 20736007), China National program (No. 2006CB932702). We thank Dr. Xin An, Jia-Qi Huang, and Guang-Hui Xu for the helpful discussion.

Appendix A. Supplementary data

Supplementary data associated with this article can be found, in the online version, at doi:10.1016/j.cattod.2009.05.018.

References

[1] G.H. Graaf, E.J. Stamhuis, A. Beenackers, Chem. Eng. Sci. 43 (1988) 3185.
[2] A.Y. Rozovskii, G.I. Lin, Top. Catal. 22 (2003) 137.
[3] J.P. Lange, Catal. Today 64 (1999) 3.
[4] X.M. Liu, G.Q. Lu, Z.F. Yan, J. Beltramini, Ind. Eng. Chem. Res. 42 (2003) 6518.
[5] C. Busetto, G. Delpiero, G. Manara, F. Trifiro, A. Vaccari, J. Catal. 85 (1984) 260.
[6] X. An, F. Ren, J.L. Li, J.F. Wang, Chin. J. Catal. 26 (2005) 729.
[7] J.P. Lange, Catal. Today 64 (2001) 3.
[8] J.L. Li, X.G. Zhang, T. Inui, Appl. Catal. A: Gen. 147 (1996) 23.
[9] J.T. Li, W.D. Zhang, L.Z. Gao, P.Y. Gu, K.Q. Sha, H.L. Wan, Appl. Catal. A: Gen. 165 (1997) 411.
[10] R.T. Figueiredo, A. Martinez-Arias, M.L. Granados, J.L.G. Fierro, J. Catal. 178 (1998) 146.
[11] U.R. Pillai, S. Deevi, Appl. Catal. B: Environ. 65 (2006) 110.
[12] X. Dong, H.B. Zhang, G.D. Lin, Y.Z. Yuan, K.R. Tsai, Catal. Lett. 85 (2003) 237.
[13] J.P. Shen, C.S. Song, Catal. Today 77 (2001) 89.
[14] I. Melian-Cabrera, M.L. Granados, J.L.G. Fierro, J. Catal. 210 (2002) 273.
[15] J. Agrell, H. Birgersson, M. Boutonnet, I. Melian-Cabrera, R.M. Navarro, J.L.G. Fierro, J. Catal. 219 (2003) 389.
[16] R.Q. Yang, X.C. Yu, Y. Zhang, W.Z. Li, N. Tsubaki, Fuel 87 (2006) 443.
[17] X. An, J.L. Li, Y.Z. Zuo, Q. Zhang, D.Z. Wang, J.F. Wang, Catal. Lett. 118 (2007) 264.
[18] R.S. Ruoff, D.C. Lorents, Carbon 33 (1995) 925.
[19] S. Berber, Y.K. Kwon, D. Tomanek, Phys. Rev. Lett. 84 (2000) 4613.
[20] H. Huang, C.H. Liu, Y. Wu, S.S. Fan, Adv. Mater. 17 (2005) 1652.
[21] C.H. Liu, H. Huang, Y. Wu, S.S. Fan, Appl. Phys. Lett. 84 (2004) 4248.
[22] B.S. Shen, X.M. Wu, H.B. Zhang, G.D. Lin, X. Dong, Acta Chim. Sin. 62 (2004) 1721.
[23] Q. Zhang, J.Q. Huang, M.Q. Zhao, W.Z. Qian, Y. Wang, F. Wei, Carbon 46 (2008) 1152.
[24] Q. Zhang, J.Q. Huang, F. Wei, G.H. Xu, Y. Wang, W.Z. Qian, D.Z. Wang, Chin. Sci. Bull. 52 (2007) 2896.
[25] R. Xiang, G. Luo, W. Qian, Y. Wang, F. Wei, Q. Li, Chem. Vapor Depos. 13 (2007) 533.
[26] Q. Zhang, G.H. Xu, J.Q. Huang, W.P. Zhou, M.Q. Zhao, Y. Wang, W.Z. Qian, F. Wei, Carbon 47 (2009) 538.
[27] X.L. Pan, Z.L. Fan, W. Chen, Y.J. Ding, H.Y. Luo, X.H. Bao, Nat. Mater. 6 (2007) 507.
[28] D.S. Su, X.W. Chen, X. Liu, J.J. Delgado, R. Schlogl, A. Gajovic, Adv. Mater. 20 (2008) 3597.
[29] J. Zhang, X. Liu, R. Blume, A.H. Zhang, R. Schlogl, D.S. Su, Science 322 (2008) 73.
[30] Q. Zhang, W.P. Zhou, W.Z. Qian, R. Xiang, J.Q. Huang, D.Z. Wang, F. Wei, J. Phys. Chem. C 111 (2007) 14638.
[31] S.M. Zhao, S.Z. Chen, F.S. Hu, Ind. Catal. 11 (2003) 26.
[32] Y.Z. Zuo, X. An, M.H. Han, J.F. Wang, D.Z. Wang, Y. Jin, Chin. J. Catal. 29 (2008) 1266.
[33] X. An, Y.Z. Zuo, Q. Zhang, D.Z. Wang, J.F. Wang, Ind. Eng. Chem. Res. 47 (2008) 6547.
[34] H.H. Kung, Catal. Today 11 (1992) 443.
[35] A.T. Aguayo, J. Erena, I. Sierra, M. Olazar, J. Bilbao, Catal. Today 106 (2005) 265.
[36] R.C. Liu, Y.Q. Yang, Y.Z. Yuan, Z.Y. Lin, C. Li, H. Yuang, Q. Wang, H.B. Zhang, J. Nat. Gas Chem. 10 (2001) 308.
[37] G.H. Graaf, H. Scholtens, E.J. Stamhuis, A. Beenackers, Chem. Eng. Sci. 45 (1990) 773.
[38] F. Deng, Q.S. Zheng, L.F. Wang, C.W. Nan, Appl. Phys. Lett. 90 (2007) 021914.
[39] C.W. Nan, Z. Shi, Y. Lin, Chem. Phys. Lett. 375 (2003) 666.
[40] Y.A. Kim, S. Kamio, T. Tajiri, T. Hayashi, S.M. Song, M. Endo, M. Terrones, M.S. Dresselhaus, Appl. Phys. Lett. 90 (2007) 093125.
[41] L. Kumari, T. Zhang, G.H. Du, W.Z. Li, Q.W. Wang, A. Datye, K.H. Wu, Compos. Sci. Technol. 68 (2008) 2178.
[42] X. Liu, Y. Zhang, A.M. Cassell, B.A. Cruden, J. Appl. Phys. 104 (2008) 084310.